Effect of Nanoparticles in Free Convection Casson Boundary Layer Flow Near a Stagnation Point Region under Microgravity Environment

Mohamad Hidayad Ahmad Kamal
Mathematical Sciences Studies, Faculty of Computer and Mathematical Sciences, Universiti Teknologi MARA (UiTM), Perak Branch, Tapah Campus

Ahmad Faiz Ahmad Shah
Mathematical Sciences Studies, Faculty of Computer and Mathematical Sciences, Universiti Teknologi MARA (UiTM), Negeri Sembilan Branch, Seremban Campus

Norshakila Abd Rasid
Mathematical Sciences Studies, Faculty of Computer and Mathematical Sciences, Universiti Teknologi MARA (UiTM), Perak Branch, Tapah Campus

Noraihan Afiqah Rawi
Department of Mathematical Sciences, Faculty of Science, Universiti Teknologi Malaysia

他

https://doi.org/10.5109/7395610

出版情報：Proceedings of International Exchange and Innovation Conference on Engineering & Sciences (IEICES). 11, pp.840-847, 2025-10-30. International Exchange and Innovation Conference on Engineering & Sciences
バージョン：

Effect of Nanoparticles in Free Convection Casson Boundary Layer Flow Near a Stagnation Point Region under Microgravity Environment

Mohamad Hidayad Ahmad Kamal[1], Ahmad Faiz Ahmad Shah[2], Norshakila Abd Rasid[1], Noraihan Afiqah Rawi[3], Sahridan Shafie[3]
[1]Mathematical Sciences Studies, Faculty of Computer and Mathematical Sciences, Universiti Teknologi MARA (UiTM), Perak Branch, Tapah Campus, 35400 Tapah Road, Perak, Malaysia
[2]Mathematical Sciences Studies, Faculty of Computer and Mathematical Sciences, Universiti Teknologi MARA (UiTM) Negeri Sembilan Branch, Seremban Campus, 70300 Seremban, Negeri Sembilan, Malaysia,
[3]Department of Mathematical Sciences, Faculty of Science, Universiti Teknologi Malaysia, 81310, Johor Bahru, Johor, Malaysia.
hidayadkamal@uitm.edu.my

Abstract: *This study investigates the g-jitter effect on three-dimensional stagnation point flow of Casson nanofluids, with a focus on understanding fluid dynamics and heat transfer under microgravity conditions. By utilizing the Tiwari-Das nanofluid model and the Keller Box method, the mathematical model develops and solves a mathematical framework to analyze critical parameters such as nanoparticle volume fraction, curvature ratio, Casson parameter, g-jitter amplitude and frequency of oscillation. Results demonstrate that the curvature ratio significantly influences velocity and heat transfer properties, enhancing the flow field around stagnation points. This study also reveals that g-jitter induces oscillatory behavior in velocity and temperature profiles, emphasizing the need for precise control in microgravity environments. Additionally, by incorporating nanoparticles into the base fluid enhances thermal conductivity, although higher concentrations increase flow resistance. The Casson parameter's variation indicates a transition towards Newtonian flow characteristics under certain conditions. The research highlights the potential for extending the analysis to other non-Newtonian fluids, hybrid nanofluids, and experimental validation in simulated microgravity conditions, thereby enriching the field of nanofluid dynamics and its applications in space and industrial contexts.*

Keywords: Boundary layer flow; Nanofluid; non-Newtonian fluid; Casson fluid; Stagnation point flow; Microgravity environment

1. INTRODUCTION

A fluid is substance of such nature that can flow and adapt its shape to the shape of its container. In the Newtonian fluids, viscosity remains constant as in the case of the different shear rate applied, which respond to Newton's law of viscosity in which the shear stress is proportional to the shear rate [1]. Non-Newtonian fluids on the other hand have changed viscosity it depends on the shear rate or stress [2]. Ren et al. [3] mention that, drilling fluids that is non-Newtonian fluids, always involve considerable yield stress and memory on the history of shearing. These fluids can display various flows behaviors like shear thinning, shear thickening and or having yield stress.

Singh et al. [4] employed viscous and elastic fluid as a non-Newtonian fluid in the analytical investigation. As the fluid is in contact with the surface or when it is moved over a solid surface, the boundary layer flow takes place for non-Newtonian fluids different from Newtonian fluid. Numerical solution for mixed variable Couette flow in the presence of buoyancy pressure was presented by Das et al. [5]. When the amount of yield stress is exceeded, the fluid acts as a Newtonian fluid with an efficient thickness.

Lots of complex mathematics fluid model was brought about due to the formulation of a new type of fluid known as nanofluid. Nanofluid a kind of new fluids with suspended nanoparticles usually has size of 1 to 100 nanometers received a large attention recently due to their interesting thermal and fluid behaviors [6]. Recently, nanotechnology has being applied in various background to solve the worldwide problem [7-10]. As small amount of nanoparticles added to the conventional base fluids, autonomously change occurs on the properties of the fluids by improving the thermal conductance, heat exchange, and viscosity of the fluid. For instance, Choi and Eastman [11] those bearing nanoscale structures to be said as ''nano liquids'' were found to possess better thermal conductivity than normal liquids. In boundary layer flow, there are two notable nanofluid model that is introduced by Buongiorno [12] and Tiwari & Das [13]; established good theoretical introductions representing pivotal data in nanofluid dynamics. Buongiorno nanofluid model's review studies on the simultaneous analysis of the various phenomena that occur in the interaction between nanoparticles and base fluids namely thermophoresis and the Brownian motion while nanofluid model introduced by Tiwari & Das involves the prediction of the enhancement of thermal conductivity and viscosity of nanofluids involving the nanoparticle volume fraction into the analysis.

Characteristics of the flow on the boundary layer is approximately altered by interaction at the boundary or impacts within the flow. Boundary layer flows emerge from an extrusion of a surface and have been widely studied [14]. An outstanding feature of boundary layer flow is the presence of stagnation points, where the velocity of the fluid relative to the surface is equal to zero and maximum pressure is experienced when the kinetic energy of fluid transform itself in to pressure energy [15]. Nadeem et al. [16] studied numerically the stagnation point flow of a non-Newtonian fluid over a stretching surface with non-orthogonal stagnation point flow.

g-Jitter define as the fluctuating gravitational field caused by crew motion and machine vibration occurs at microgravity environment. Rawi et al. [17] numerically investigate the influence of g-jitter on Jeffrey fluid flow over a sheet and analyzed the influence of g-jitter merged convection second grade nanofluid on a sheet stretched diagonally keeping in view all aspects of the nanoparticles using Keller box method. The study shown shape of nanoparticles plays a critical role in determining the thermal and flow behavior in non-Newtonian nanofluids.

By considering the research background conducted on boundary layer Casson fluid flow associated with the incorporation of the developed Tiwari and Das nanofluid model and effect of stagnation points and g-jitter, this study proposed a fundamental study on the effect of Casson nanofluid flow in fluid behaviors and thermal characteristic. By mathematically formulating the fluid flow based on the fluid configuration and effects considered, a system of partial differential equation introduced and later solved and analyzed numerically using finite different approach. The analysis results based on the effect considered then presented graphically in term of velocity and temperature profile that represent the flow behaviors and thermal characteristic respectively.

2. MATHEMATICAL FORMULATION

Unsteady free convection Casson nanofluid flow induced by g-jitter effect near a three-dimensional stagnation point region is considered. A nodal point stagnation point is denoted as **N**, represent the geometrical shape of the body. The temperature of boundary body is assumed to be constant and denoted by T_W while T_∞ is the temperature of the fluid in the free stream. The $x-$and $y-$ coordinates are measured along the body surface, while the $z-$coordinate is measured normal to the body surface. By considering all of this effect, a system of partial differential equation is mathematically formulated based on physical law and principle into continuity, momentum and heat equation takes a form as [18-19]

$$\frac{\partial u}{\partial x}+\frac{\partial v}{\partial y}+\frac{\partial w}{\partial z}=0, \tag{2.1}$$

$$\begin{gathered}\rho_{nf}\left(\frac{\partial u}{\partial t}+u\frac{\partial u}{\partial x}+v\frac{\partial u}{\partial y}+w\frac{\partial u}{\partial z}\right)= \\ g_0\left[1+\varepsilon\cos\left(\pi\omega t\right)\right]\left(\rho\beta_t\right)_{nf}ax\left(T-T_\infty\right) \\ +\mu_{nf}\left(1+\frac{1}{\beta}\right)\frac{\partial^2 u}{\partial z^2},\end{gathered} \tag{2.2}$$

$$\begin{gathered}\rho_{nf}\left(\frac{\partial v}{\partial t}+u\frac{\partial v}{\partial x}+v\frac{\partial v}{\partial y}+w\frac{\partial v}{\partial z}\right)= \\ g_0\left[1+\varepsilon\cos\left(\pi\omega t\right)\right]\left(\rho\beta_t\right)_{nf}by\left(T-T_\infty\right) \\ +\mu_{nf}\left(1+\frac{1}{\beta}\right)\frac{\partial^2 v}{\partial z^2},\end{gathered} \tag{2.3}$$

$$\frac{\partial T}{\partial t}+u\frac{\partial T}{\partial x}+v\frac{\partial T}{\partial y}+w\frac{\partial T}{\partial z}=\alpha_{nf}\frac{\partial^2 T}{\partial z^2}, \tag{2.4}$$

subjected to

$$\begin{aligned}&u=v=w=0,\ T=T_\infty \text{ for any } x, y \text{ and } z,\\&u=v=w=0,\ T=T_w \text{ on } z=0,\ x\ge 0,\ y\ge 0,\\&u=v=0,\qquad T=T_\infty \text{ on } x=0,\ y\ge 0,\ z\ge 0,\\&u=v=0,\qquad T=T_\infty \text{ on } y=0,\ x\ge 0,\ z\ge 0,\\&u=v\to 0,\qquad T=T_\infty \text{ as } z\to 0, x\ge 0,\ y\ge 0.\end{aligned} \tag{2.5}$$

Parameter u,v and w are the velocity element in the direction of x,y,z axes respectively. T is the dimensional temperature parameter of the nanofluid. The thermophysical properties of the nanofluid are carried by subscribing with a term nf whereas $\rho,\ \mu,\ \beta_t\ \alpha$ and C_p denote the density, dynamic viscosity, thermal expansion, thermal diffusion, and specific heat capacity at constant pressure. Here, the stagnation point flow characteristics are defined in terms of parameters a and b which are the principal curvature measured on the stagnation point at the $x=0$ and $y=0$ plane. Parameter β is a dimensionless Casson parameter that describes the flow behaviour of non-Newtonian fluids, particularly in shear-thinning fluids. This system of equation is in dimensional form where the unit of each parameter considered may affect the effectiveness of calculation later. To reduce the complexity of the system partial differential equation, semi-similar transformation will be applied using the semi similar variables [18],

$$\begin{aligned}&\eta=Gr^{1/4}az,\ \tau=\Omega t,\ t=\nu a^2Gr^{1/2}t^*,\\&u=\nu a^2xGr^{1/2}f',\ v=\nu a^2yGr^{1/2}h',\\&w=-\nu aGr^{1/4}\left(f+h\right),\\&\Omega=\frac{\omega}{\nu a^2Gr^{1/2}},\quad \theta=\frac{\left(T-T_\infty\right)}{\left(T_w-T_\infty\right)},\\&Gr=\frac{g_0\beta_t\left(T-T_\infty\right)}{a^3\nu^2},\end{aligned} \tag{2.6}$$

where ν is the kinematic viscosity of the fluid and Gr is the thermal Grashof numbers. Notation f and h is the dimensionless function with f' and h' is the dimensionless velocity in $x-$ and $y-$ direction respectively. The prime notation at the top of the function f and h indicate the differentiation with respect to η. Here, θ and Ω are the dimensionless variables for temperature, and frequency of oscillation. The expressions of nanofluid constants for nanofluid are defined as [18],

$$\mu_{nf} = \frac{1}{(1-\phi)^{2.5}}, \alpha_{nf} = \frac{k_{nf}}{(\rho C_p)_{nf}},$$
$$\rho_{nf} = (1-\phi)\rho_f + \phi\rho_s,$$
$$\frac{k_{nf}}{k_f} = \frac{(k_s + 2k_f) - 2\phi(k_f - k_s)}{(k_s + 2k_f) + \phi(k_f - k_s)}, \tag{2.7}$$
$$(\rho\beta_t)_{nf} = (1-\phi)(\rho\beta_t)_f + \phi(\rho\beta_t)_s,$$
$$(\rho C_p)_{nf} = (1-\phi)(\rho C_p)_f + \phi(\rho C_p)_s.$$

Here, ϕ is defined as the nanoparticle volume fraction which is the concentration of the nanoparticles that is added into the fluid and k is defined as the thermal conductivity. The subscript f and s represent the fluid and solid component in the nanofluid mixture respectively. By using semi-similar variables in (2.6) and nanofluid constant in (2.7), the system of the partial differential equation (2.1) – (2.5) will be transformed into dimensionless governing equations such that,

$$\left(1-\phi+\phi\frac{\rho_s}{\rho_f}\right)\left(\Omega\frac{\partial f'}{\partial \tau}\right) = \frac{f'''}{(1-\phi)^{2.5}}\left(1+\frac{1}{\beta}\right) + \left[1-\phi+\frac{\phi(\rho\beta_t)_s}{(\rho\beta_t)_f}\right]\left[1+\varepsilon\cos(\pi\tau)\right] + \left(1-\phi+\phi\frac{\rho_s}{\rho_f}\right)\left[(f+h)f''-f'^2\right], \tag{2.8}$$

$$\left(1-\phi+\phi\frac{\rho_s}{\rho_f}\right)\left(\Omega\frac{\partial h'}{\partial \tau}\right) = \frac{h'''}{(1-\phi)^{2.5}}\left(1+\frac{1}{\beta}\right) + \left[1-\phi+\frac{\phi(\rho\beta_t)_s}{(\rho\beta_t)_f}\right]\left[1+\varepsilon\cos(\pi\tau)\right] + c\left(1-\phi+\phi\frac{\rho_s}{\rho_f}\right)\left[(f+h)h''-h'^2\right], \tag{2.9}$$

$$\frac{1}{\Pr}\frac{\left[\frac{(k_s-2k_f)-2\phi(k_f-k_s)}{(k_s-2k_f)+\phi(k_f-k_s)}\right]}{\left[(1-\phi)+\frac{\phi(\rho C_p)_s}{(\rho C_p)_f}\right]}\theta'' + (f+h)\theta' = \Omega\frac{\partial\theta}{\partial\tau}, \tag{2.10}$$

subjected to

$$f(\eta,0) = f'(\eta,0) = 0,$$
$$h(\eta,0) = h'(\eta,0) = 0, \quad \theta(\eta,0) = 1, \tag{2.11}$$
$$f' \to 0, \; h' \to 0, \; \theta \to 0, \; \text{as} \; \eta \to \infty$$

The system of dimensionless equations in (2.8) – (2.10) together with dimensionless initial and boundary condition (2.11) are then solve numerically using implicit finite different approach method known as Keller box method.

3. RESULTS AND DISCUSSION

Previous section successfully discusses on reducing the complexity of the system of partial differential equation using semi-similar transformation technique. The dimensionless system of equation is then solved numerically using implicit finite different approach known as Keller box method. Copper (Cu) nanoparticle and carboxymethyl cellulose (CMC) as the base fluid was use in this problem. Details of thermophysical quantities of Cu and CMC are shown in Table 1.

Fig. 1 – Fig. 21 shown the results of profiles either velocity profile in the $x-$direction, velocity profile in $y-$ direction and temperature profile. All the profiles presenting the natural convection flow behaviour and satisfying the boundary condition in (2.11) that also validating the collected results. The analysis conducted is to determination effect of curvature ratio c, amplitude of modulation ε, frequency of oscillation Ω, Casson parameter β and nanoparticle volume fraction ϕ on the flow behaviour and thermal characteristics.

Table 1. Thermophysical quantities of the nanoparticles and base fluid

Physical Properties	Copper (Cu)	Carboxymethyl Cellulose (CMC)
Density	8933	997.1
Specific heat capacity	385	4179
Thermal conductivity	401	0.613
Thermal expansion	1.67	21

The analysis of curvature ratio parameter that represent stagnation point parameter analysed in Fig. 1 – Fig. 3 for $c=0$, Fig. 4 – Fig. 6 for $c=0.5$ and Fig. 7 – Fig. 9 with $c=1.0$. By comparing the results of velocity profile, a decreasing behaviour is noticed on the velocity profile in $x-$direction as the curvature ratio parameter increases while a contradict behaviour on $y-$ direction. The curvature ratio defines as a dimensionless parameter used in fluid dynamics to quantify the effect of surface curvature on fluid flow. The increases of curvature ratio parameter represent more geometric resistance along $x-$ direction while less restrictive in $y-$ direction. Thus, increasing of curvature ratio parameter decrease the velocity profile in $x-$ direction while contradict behaviour occurs on velocity profile in $y-$ direction. Another interesting finding in this effect is at $c=0$, there fluid is remained at rest in $y-$ direction as shown in Fig. 2 regardless of various parameter value of amplitude of modulation induced. In addition, an exactly similar velocity profile in $x-$ and $y-$ direction were noticed in Fig.7 and Fig.8 respectively as curvature ratio parameter value $c=1.0$ was applied. The value of curvature ratio represents the geometrical shape of the boundary body with $c=0$ represent cylindrical shape and $c=1.0$ is a spherical shape of boundary body. In stagnation point flow, fluid behaviour as illustrate in Fig. 2 known as plane stagnation point flow while fluid behaviour in Fig. 7 and Fig. 8 known as axisymmetric stagnation point

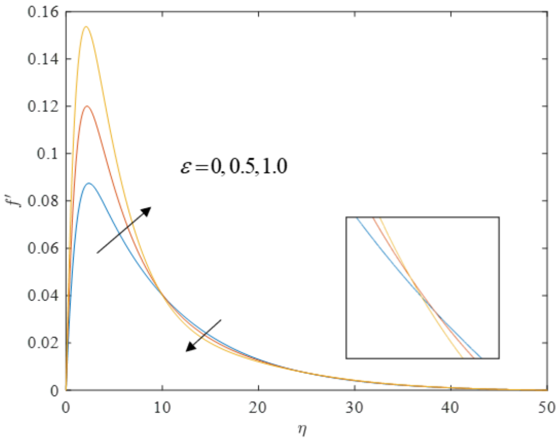

Fig. 1. Effect of ε on velocity profile in $x-$directions with $\phi = 0.02, \Omega = 0.2$ while $c=0$.

flow. Thus, cylindrical boundary body produced plane stagnation point flow while spherical boundary body produced axisymmetric stagnation point flow pattern.

Fig. 10 – Fig.12 presenting the results of velocity and temperature profile with various values of amplitude of modulation ε, apply. Amplitude of modulation is one of the parameters that measure the effect of g-jitter that occurs under microgravity environment with the amplitude of modulation measured the maximum

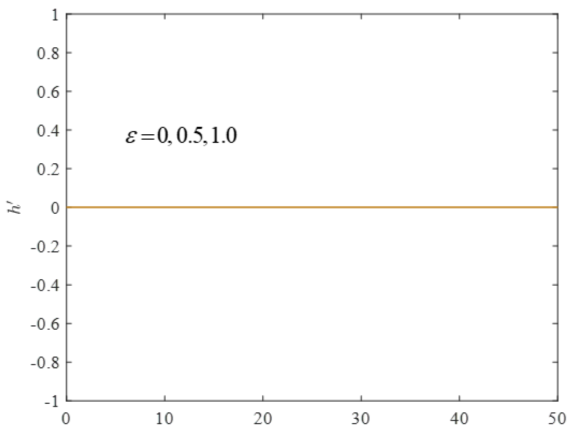

Fig. 2. Effect of ε on velocity profile in $y-$directions with $\phi = 0.02, \Omega = 0.2$ while $c=0$.

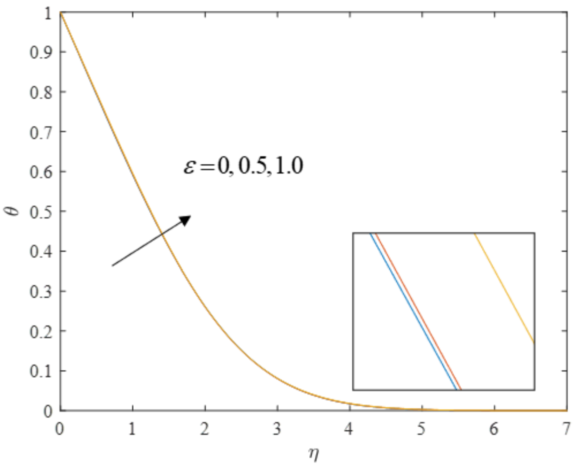

Fig. 3. Effect of ε on temperature profile with $\phi = 0.02, \Omega = 0.2$ while $c=0$.

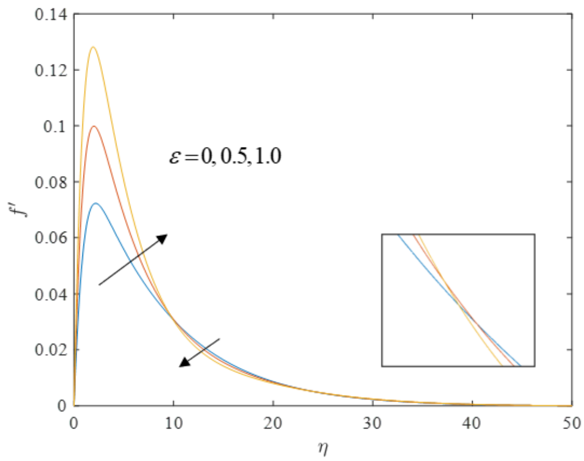

Fig. 4. Effect of ε on velocity profile in $x-$directions with $\phi = 0.02, \Omega = 0.2$ while $c=0.5$.

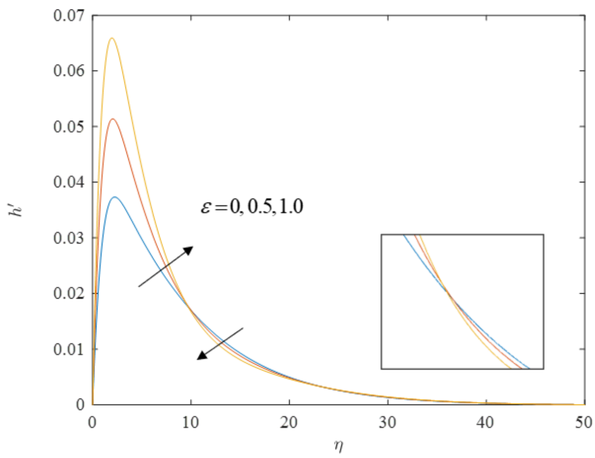

Fig. 5. Effect of ε on velocity profile in $y-$directions with $\phi = 0.02, \Omega = 0.2$ while $c=0.5$.

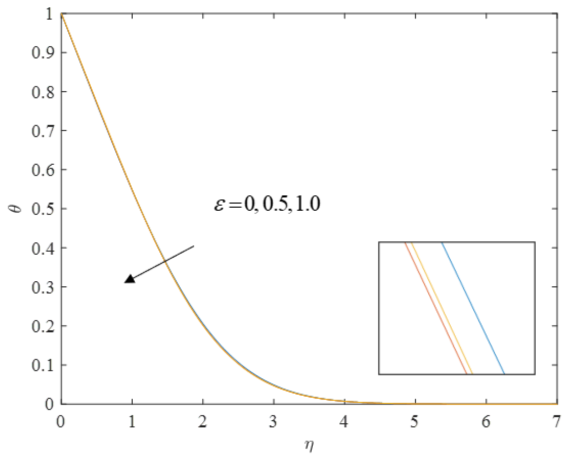

Fig. 6. Effect of ε on temperature profile with $\phi = 0.02, \Omega = 0.2$ while $c = 0.5$.

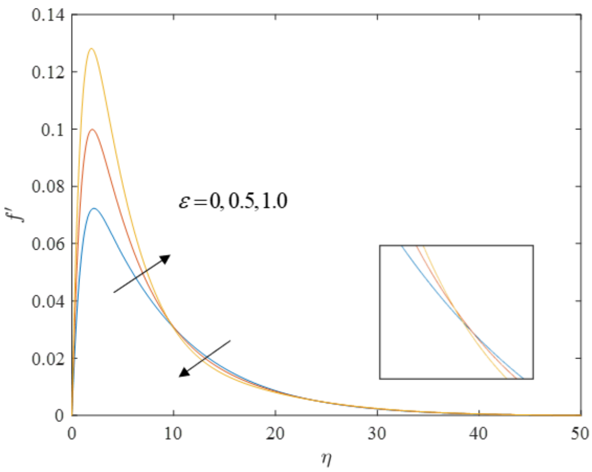

Fig. 7. Effect of ε on velocity profile in $x-$directions with $\phi = 0.02, \Omega = 0.2$ while $c = 1.0$.

strength of the fluctuating acceleration caused by g-jitter in a microgravity environment. From the figure, the increases of ε cause greater fluctuating effect compared to small value of ε with $\varepsilon = 0$ shows perfect microgravity, with no periodic shaking or vibration influencing the flow. A higher amplitude of modulation in g-jitter injects more energy into the fluid system at each cycle, causing larger deviations from steady-state flow and producing more fluctuating velocity profiles.

Other than amplitude of modulation, another parameter that measure the existence of g-jitter effect are known as frequency of oscillation, Ω. Fig. 4 – Fig. 6 illustrate the profiles when low frequency of oscillation induced while Fig. 13 – Fig. 15 shown higher frequency of oscillation. The results show that, the number of fluctuations occurs more frequently on the higher frequency of oscillation compared to lower frequency of oscillation. In addition,

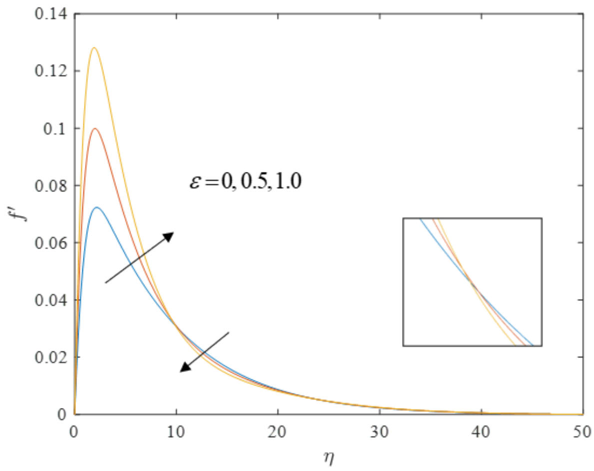

Fig. 8. Effect of ε on velocity profile in $y-$directions with $\phi = 0.02, \Omega = 0.2$ while $c = 1.0$.

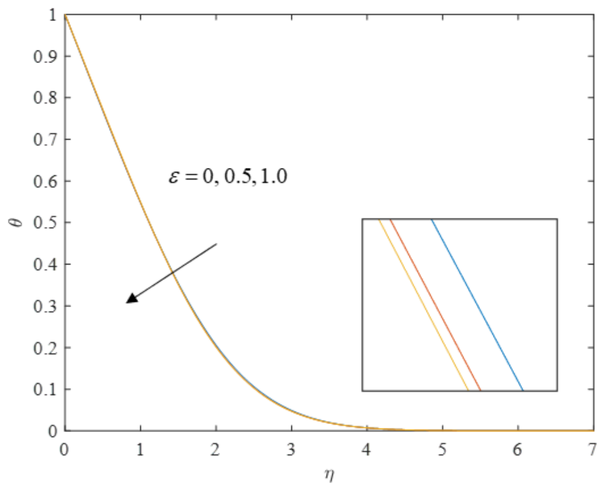

Fig. 9. Effect of ε on temperature profile with $\phi = 0.02, \Omega = 0.2$ while $c = 1.0$.

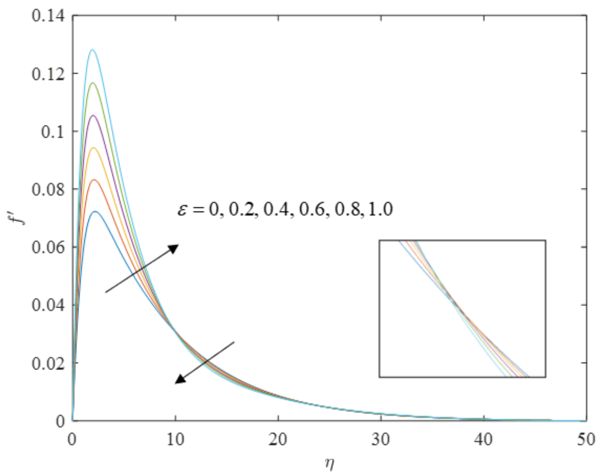

Fig. 10. Effect of ε on velocity profile in $x-$directions with $\phi = 0.02, \Omega = 0.2$ while $c = 0.5$.

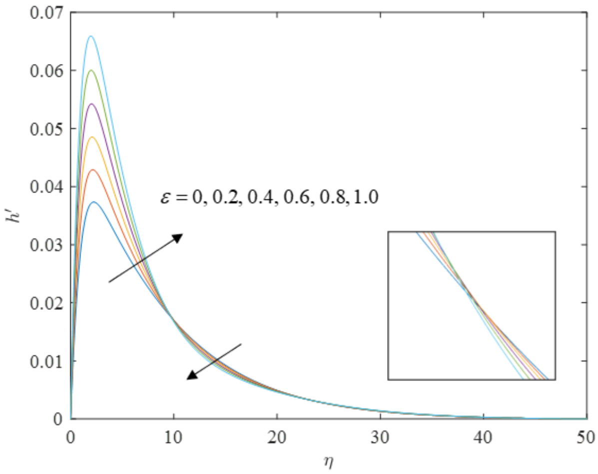

Fig. 11. Effect of ε on velocity profile in $y-$ directions with $\phi = 0.02, \Omega = 0.2$ while $c = 0.5$.

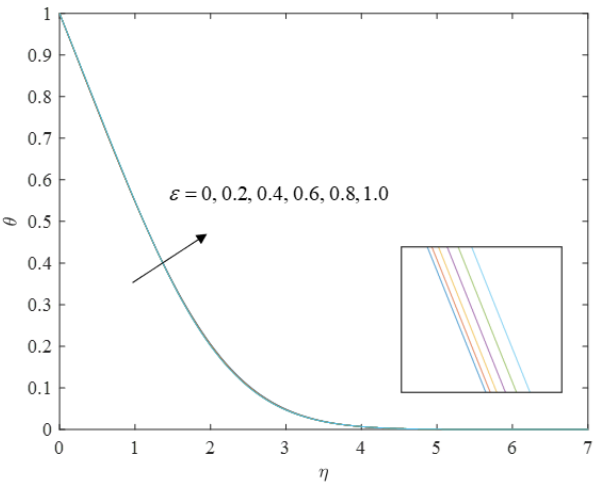

Fig. 12. Effect of ε on temperature profile with $\phi = 0.02, \Omega = 0.2$ while $c = 0.5$.

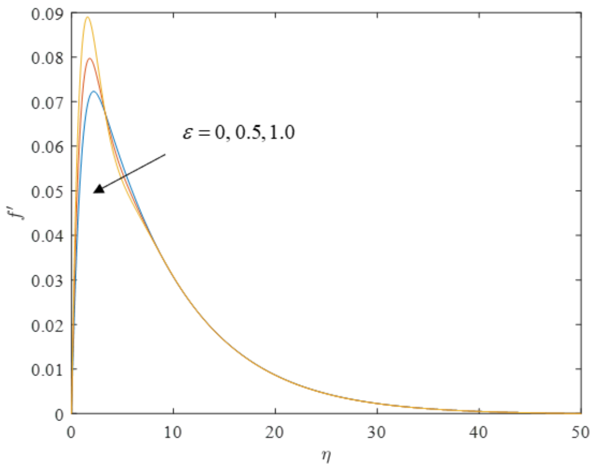

Fig. 13. Effect of ε on velocity profile in $x-$ directions with $\phi = 0.02, \Omega = 2.0$ while $c = 0.5$.

the effect of ε was also found to be less significant on the higher Ω. It shows that Ω plays a key role in determining the dynamic response of the fluid to microgravity disturbances.

Fig. 16 – Fig. 18 illustrate the effect of Casson parameter β, on velocity and temperature profiles. Casson parameter characterizes the non-Newtonian behaviour of Casson fluids, a type of shear-thinning fluid that behaves like a solid until a certain yield stress is exceeded. Low value of β means strong yield stress effects, while a high value means the fluid behaves more like a Newtonian fluid. From the figure, the increases of β decrease both velocity profiles and temperature profile. In addition, the thickness of boundary layer for both velocity and temperature profile also decrease as β

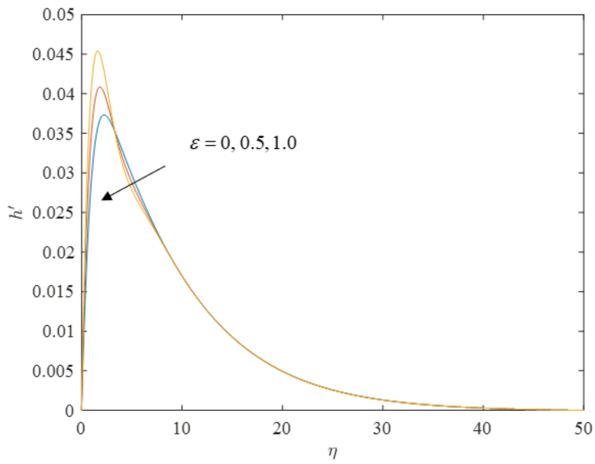

Fig. 14. Effect of ε on velocity profile in $y-$ directions with $\phi = 0.02, \Omega = 2.0$ while $c = 0.5$.

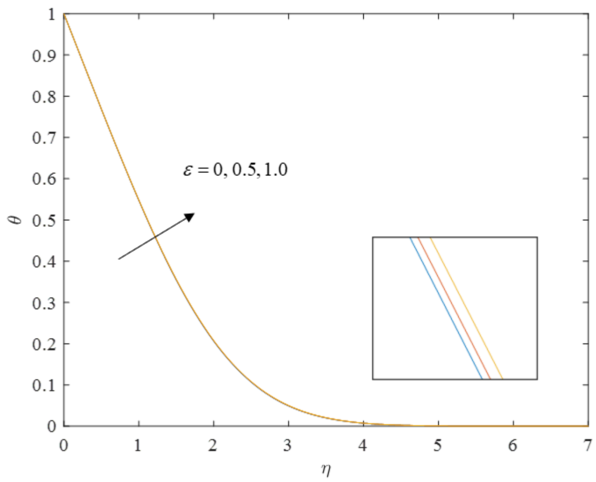

Fig. 15. Effect of ε on temperature profile with $\phi = 0.02, \Omega = 2.0$ while $c = 0.5$.

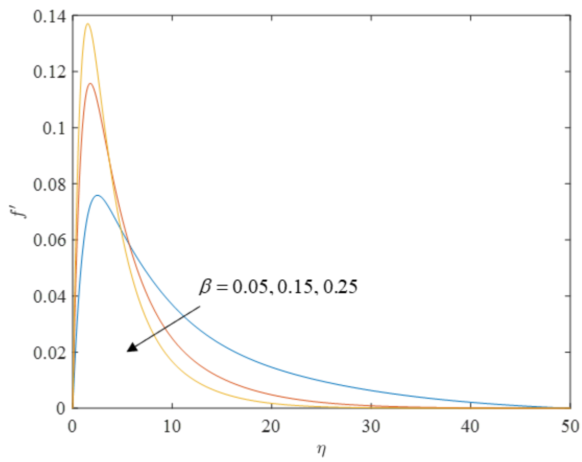

Fig. 16. Effect of β on velocity profile in $x-$directions with $\phi = 0.02, \Omega = 0.2$ while $c = 0.5$.

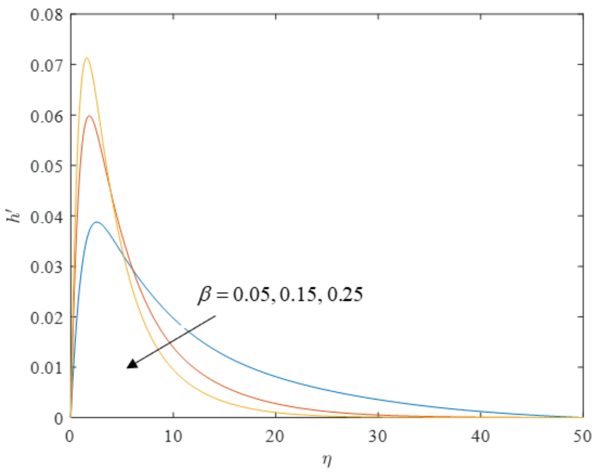

Fig. 17. Effect of β on velocity profile in $y-$directions with $\phi = 0.02, \Omega = 0.2$ while $c = 0.5$.

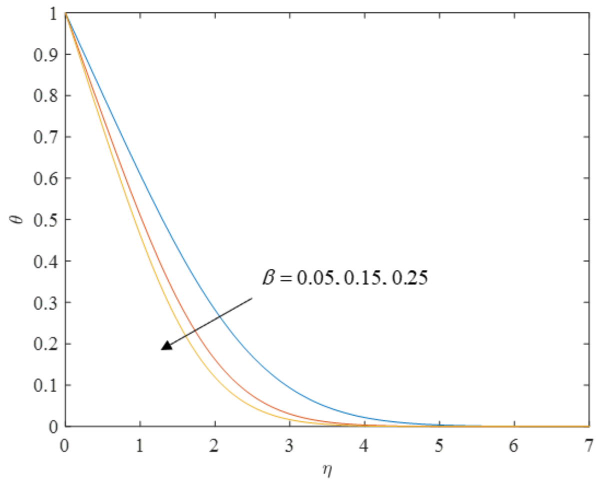

Fig. 18. Effect of β on temperature profile with $\phi = 0.02, \Omega = 0.2$ while $c = 0.5$.

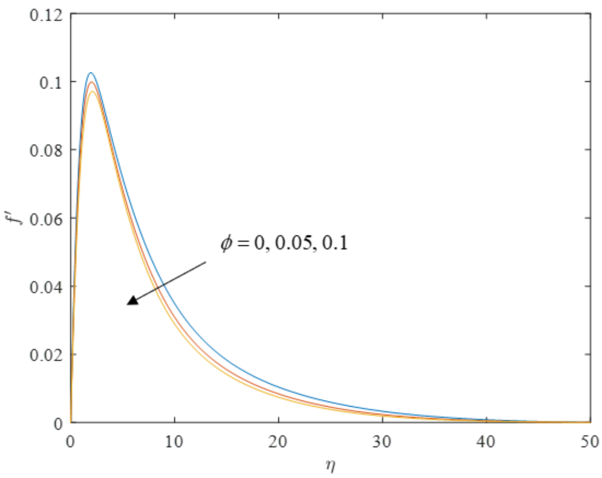

Fig. 19. Effect of ϕ on velocity profile in $x-$directions with $\beta = 0.05, \Omega = 0.2$ while $c = 0.5$.

value increase. Since the Casson parameter is inversely related to the yield stress of the fluid, lower effective viscosity was contributed from this yield stress. An increase in the Casson parameter reduces the influence of yield stress but increases the overall resistance to flow and heat transport, resulting in lower velocity and temperature profiles in the boundary layer.

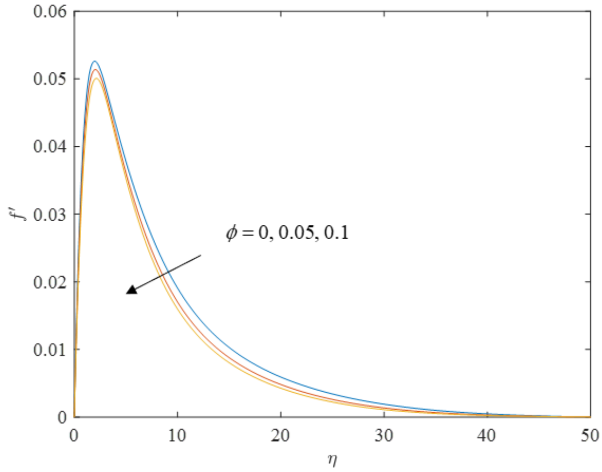

Fig. 20. Effect of ϕ on velocity profile in $y-$directions with $\beta = 0.05, \Omega = 0.2$ while $c = 0.5$.

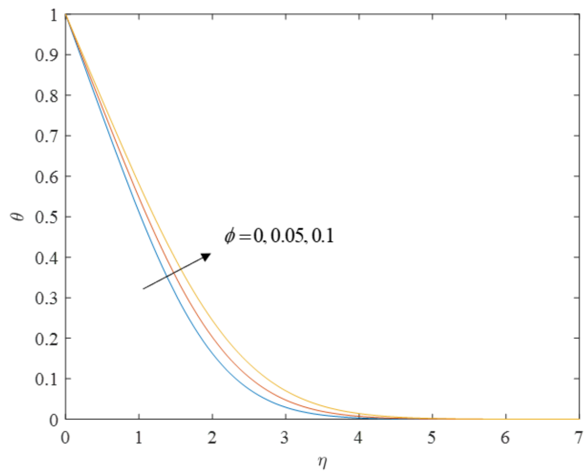

Fig. 21. Effect of ϕ on temperature profile with $\beta = 0.05, \Omega = 0.2$ while $c = 0.5$.

Nanoparticle volume fraction ϕ, defines as ratio of the volume of nanoparticles to the total volume of the nanofluid mixture and this effect are analysed in Fig. 19 – Fig. 21 in term of velocity and temperature profile. The analysis shows that increases of ϕ increase the temperature profile but decrease the velocity profile in both directions. Increases of ϕ parameter value indicates the increases of volume of nanoparticle in the nanofluid mixture. Adding nanoparticles to a base fluid increases the effective dynamic viscosity of the nanofluid that in which more viscous fluid produces greater resistance to flow. On the other hand, nanoparticles have much higher thermal conductivity than base fluids which then enhances the effective thermal conductivity of the fluid system. Thus, as the nanoparticle volume fraction increases, the fluid becomes more viscous and more thermally conductive, leading to a slower but hotter fluid flow.

4. CONCLUSION

A theoretical study on free convection Casson nanofluid flow near a three-dimensional stagnation point region was successfully conducted subjected to constant wall boundary condition. The problem was mathematically formulated into a system of partial differential equation and solved using finite different approach namely Keller box method. From the study, by considering the effect such as g-jitter, stagnation point, nanofluid and Casson fluid, the analysis of these effect can be summarised as below,

i. Higher ε causes stronger fluctuations in both velocity and temperature profiles.
ii. Higher Ω increases the number of fluctuations in the velocity and temperature profiles.
iii. Higher β reduces velocity and temperature profiles and thins both momentum and thermal boundary layers.
iv. Increasing ϕ decreases velocity profile due to increased viscosity but increases temperature profile due to enhanced thermal conductivity.

5. ACKNOWLEDGEMENT

The authors would like to thanks Ministry of Higher Education Malaysia for providing financial support under the Fundamental Research Grant Scheme (FRGS-EC) FRGS-EC/1/2024/STG06/UITM/02/18

6. REFERENCES

[1] L. Yunzi, K. R. Ward, M. A. Burns, Viscosity measurements using microfluidic droplet length, Analytical Chemistry, 89(7) (2017) 3996-4006

[2] Rajagopal, R. Kumbakonam, Mechanics of non–Newtonian fluids (Eds.), Recent Developments in Theoretical Fluid Mechanics, Chapman and Hall/CRC, London, 2023, pp. 129-162.

[3] R. Jiangtao, Y. Deshun, R. Zhai, Rheological behavior of bentonite-water suspension at various temperatures: Effect of solution salinity, Engineering Geology 295 (2021), 106435.

[4] J. Singh, M. Rudman, and H. M. Blackburn, The effect of yield stress on pipe flow turbulence for generalised Newtonian fluids, Journal of Non-Newtonian Fluid Mechanics 249 (2017) 53-62.

[5] S. Das, R. N. Jana, O. D. Makinde, Magnetohydrodynamic mixed convective slip flow over an inclined porous plate with viscous dissipation and Joule heating, Alexandria Engineering Journal 54(2), (2015) 251-261.

[6] D. D. Kumar, V. A. Amirtham, A review on preparation, characterization, properties and applications of nanofluids, Renewable and Sustainable Energy Reviews 60 (2016) 21-40.

[7] S. Hossain, Recent advances with CNT, nanocellulose and their composites in different industries, in Proceedings of International Exchange and Innovation Conference on Engineering & Sciences (IEICES) 9 (Kyushu University, 19 October 2023) 123 - 130. IEICES website: https://catalog.lib.kyushu-u.ac.jp/opac_download_md/7157962/2023_p123.pdf (accessed 26.05.2025)

[8] N. Neogi, K. P. Choudhury, Utilization of metal-based nanoparticles in biomedical imaging technologies, in Proceedings of International Exchange and Innovation Conference on Engineering & Sciences (IEICES) 9 (Kyushu University, 19 October 2023) 65 - 71. IEICES website: https://catalog.lib.kyushu-u.ac.jp/opac_download_md/7157949/2023_p065.pdf (accessed 26.05.2025)

[9] U. N. Eldemerdash, Advances in chemical enhanced oil recovery using nanofluids. in Proceedings of International Exchange and Innovation Conference on Engineering & Sciences (IEICES) 9 (Kyushu University, 19 October 2023) 26 - 27. IEICES website: https://catalog.lib.kyushu-u.ac.jp/opac_download_md/7157929/2023keynotespeaker_Eldmerdash.pdf (accessed 26.05.2025)

[10] A. I. Helal, N. Neogi, K. P. Choudhury, MD. G. Sazid, An analysis of the photocatalytic activities of ZnO nanoparticles: Factors influencing dye degradation, in Proceedings of International Exchange and Innovation Conference on Engineering & Sciences (IEICES) 9 (Kyushu University, 19 October 2023) 21 - 27. IEICES website: https://catalog.lib.kyushu-u.ac.jp/opac_download_md/7157937/2023_p021.pdf (accessed 26.05.2025)

[11] S. U. S. Choi, J. A. Eastman, Enhancing thermal conductivity of fluids with nanoparticles in ASME International Mechanical Engineering Congress & Exposition, (San Francisco, 01 October 1995)

[12] J. Buongiorno, Convective transport in nanofluids, J. Heat Transfer 128(3) (2006) 240 - 250.

[13] R. K. Tiwari, M. K. Das, Heat transfer augmentation in a two-sided lid-driven differentially heated square cavity utilizing nanofluids, Int. J. Heat and Mass Transfer, 50(9–10) (2007) 2002 – 2018.

[14] B. C. Sakiadis, Boundary-layer behavior on continuous solid surfaces: II. The boundary layer on a continuous flat surface. AIChE J., 7 (1961) 221-225.

[15] S. Chander, A. Ray, An experimental and numerical study of stagnation point heat transfer for methane/air laminar flame impinging on a flat surface, Int. J. Heat and Mass Transfer 51(13-14) (2008) 3595-3607.

[16] S. Nadeem, R. Mehmood, N. S. Akbar, Non-orthogonal stagnation point flow of a nano non-Newtonian fluid towards a stretching surface with heat transfer, Int. J. Heat and Mass Transfer, 57(2) (2013) 679–689.

[17] N. A. Rawi, M. R. Ilias, Z. M. Isa, S. Shafie, Sharidan. (2017). Effect of gravity modulation on mixed convection flow of second grade fluid with different shapes of nanoparticles, Malaysian Journal of Fundamental and Applied Sciences, 13 (2017) 10.11113

[18] M. H. A. Kamal, A. Ali, S. Shafie. g-Jitter free convection flow of nanofluid in the three-dimensional stagnation point region, MATEMATIKA, (2019) 260-270.

[19] S. Nadeem, R. U. Haq, N. S. Akbar, MHD three-dimensional boundary layer flow of Casson nanofluid past a linearly stretching sheet with convective boundary condition. IEEE Transactions on Nanotechnology 13(1) (2013) 109-115.